

# Photophysical studies of probes bound to cross-link junctions in poly(dimethyl siloxane) elastomers and nanocomposites

Pieter B. Leezenberg<sup>2</sup>, M. D. Fayer<sup>3</sup> and Curtis W. Frank<sup>1\*</sup>

Departments of Chemical Engineering<sup>1</sup>, Materials Science and Engineering<sup>2</sup> and Chemistry<sup>3</sup>, Stanford University, Stanford, CA 94305-5025, USA

**Abstract:** Naphthalene and dansyl chromophores are covalently attached to trifunctional cross-link junctions in poly(dimethyl siloxane) elastomers. Photophysical measurements are subsequently used to monitor the junction dynamics in unfilled elastomers and the local junction environment in nanocomposites prepared by sol-gel *in-situ* precipitation techniques. Transient fluorescence anisotropy measurements of the naphthalene chromophore are interpreted in terms of a fast, partial reorientation within a restricted cone and a slow, complete reorientation driven by cooperative motions of larger chain segments connected to the cross-link. Steady state fluorescence measurements of the dansyl chromophore in unfilled elastomers and in silica-containing nanocomposites suggest the existence of two populations of chromophores: one that is tightly immobilized through interactions with inorganic domains and a second that is free to move within the elastomeric domain.

## INTRODUCTION

Poly(dimethyl siloxane) (PDMS) elastomers have been widely studied because they retain their useful mechanical and electrical properties over a temperature range from below 173K to above 573K. They have good thermal, oxidative and hydrolytic stability, and are resistant to changes in pH (1). These properties arise because of the dramatic flexibility provided by the siloxane bond, causing the dynamic properties of PDMS systems to be of particular fundamental interest. In most technological applications, PDMS elastomers contain a number of additives, such as reinforcing fillers, antioxidants, and dyes (1-3). Some types of rigid filler particles can reinforce the network, resulting in improved modulus, tensile strength and toughness (4) as well as less desirable characteristics including increased relaxation and creep rates, heat aging, stress softening and compression or tensile set. The traditional way of incorporating filler into the rubber is to mechanically stir silica particles into the reagents prior to curing the network (5). However, it is difficult to obtain homogeneous dispersion by this procedure, and the increase in viscosity during cure requires a large energy input for mixing. An alternative process to reinforce PDMS elastomers is to employ sol-gel techniques and precipitate alkoxysilanes *in situ* inside the polymer matrix, yielding a "nanocomposite" (3, 6-9). This allows easy control over the size, structure and dispersion of the silica phase. In this paper, we describe the use of naphthalene and dansyl probe molecules attached to cross-link junctions of model PDMS networks. We use the fluorescence signal from labeled networks to monitor the dynamics of motion of the junction in the unfilled elastomer and the local environment of the cross-link junction in a nanocomposite system, respectively.

## BACKGROUND

In the following, we describe the relevant structural and dynamic aspects of elastomeric and nanocomposite materials in order to identify the molecular phenomena of interest for study by attachment of functional dyes. We pay particular attention to the role of the cross-link junction, in anticipation of the discussion of our photophysical measurements on junction-labeled PDMS networks.

### Molecular Theories of Rubber Elasticity

An ideal network is composed of a system of  $f$  network chains emanating from each of the  $f$ -functional cross-link junctions and terminating in other cross-link junctions. The network is infinite in extent with no dangling chain ends, loops or unreacted chains. Central to much of the theoretical work related to rubber elasticity is the behavior of the cross-link junctions. The earliest approaches to explain the molecular origin of rubber elasticity were the affine and the phantom network models. In the affine network model (10), the cross-link junctions do not fluctuate around a mean position and they move affinely with strain. The mean square fluctuations in junction position are zero. The phantom network model assumes that network chains can freely pass through each other, i.e. no intermolecular

interactions occur. Network chains respond to external perturbations only through their ends connected to cross-link junctions. The mean locations of the cross-links move with macroscopic deformation, while the instantaneous deviations do not. The two models are currently believed to be extreme cases: the affine network model is approached at low deformation, whereas the phantom network model is a better approximation at higher deformation.

Flory (11) has proposed a constrained junction model that permits a gradual transition between affine and phantom behavior. In real networks at small deformations, cross-links do fluctuate but not as much as in the phantom model. Flory argues (11-14) that the cross-link junctions are most vulnerable to entanglements and constraints since each of them connects  $f$  chains to it. This is contrary to the Graessley model (15), which argues that, in the limit of small strain, the interactions along the chain contour do contribute to the modulus. Fluctuations of the junction are constrained by the involvement of the  $f$  chains extending from it. Both the Graessley and Flory models account for the intermediate behavior of the modulus of a real network between the phantom and affine limits. Thus, in the affine, phantom and constrained junction models, which are all considered to be junction fluctuation theories (16), the mobility of the cross-link junction is of crucial importance in determining the modulus.

Alternate approaches are given by the slip-link and primitive path models. They are based on the tube model for polymer melts, which assumes that large scale motions of the chain are severely hindered by non-permanent entanglements, and the polymer chain reptates in a tube formed by entanglements along its own contour (17). In elastomers the chains are connected at both ends so they cannot freely reptate, and the tube is fixed. Entanglements in the uncross-linked polymer chains are trapped during the curing process, which results in "slip-links" along the network chains. At low deformation, the slippage of entanglements between cross-links is the dominant deformation mechanism (18). The slip-link model has been moderately successful in predicting experimental extension data (16,19).

At larger deformations the primitive path model of Edwards (19-21) gives a better description. In this model, all the entanglements along the chain are taken into account, instead of only one as in the case of the slip-link model. In real networks, many slip-links are trapped between two cross-links. The entanglements create a tube resulting in a "primitive path" of random walk that is shorter than the contour length of a chain. A new length scale is introduced, given by the average distance between entanglements, which is also the distance that an entanglement can slide along the chain contour.

### Network Dynamics

Chain segments and cross-link junctions in rubber networks are subject to random Brownian motion (17,22). Since motions of polymer chains occur on a range of time and distance scales (17,22,23), the motion of the cross-links is also heterogeneous and has to be described by a distribution of correlation times. In the following, we review the relationship between  $f$  and the dynamic motions of the cross-link junctions. Later, we describe our use of fluorescence depolarization of a naphthyl group covalently attached to the cross-link junction to obtain direct experimental information about the dynamics.

In the phantom network, the translational diffusive motions of a cross-link junction are related to  $\langle r^2 \rangle$ . In Flory's constrained junction theory, the diffusive motions of the junctions are more constrained than in the phantom model. In the affine model, diffusive cross-link motions are completely restrained to zero. Warner (16,24,25) calculated an expression for the translational diffusion coefficient of the  $f$ -functional cross-links. Warner and Edwards (26) also predicted the scattering cross section for networks in the framework of the localization model by Deam and Edwards (20). This analysis is only valid for small scale ( $<30 \text{ \AA}$ ) and short time dynamics, where the latter constraint implies that the time is too short for neighboring cross-links or entanglements to interfere and introduce additional correlations into the dynamics. These predictions were tested by Higgins (27) using high resolution small angle neutron scattering. The results confirmed the slowing down of the rate of motion of a  $f$ -connected point relative to a freely moving point.

There is no well-established model that describes the long-time dynamics of networks, but a number of hypotheses have been suggested. A correlation has been found between the characteristic relaxation time and the number of defects in a network, in particular the dangling chains. A reptation mechanism that describes diffusion of these dangling chains has been suggested by Curro and Pincus (28). However, they neglected the dynamics of the rest of the network. Neuberger and Eichinger (29) suggested that the slow modes are associated with small entropic force constants in the equations for the Rouse dynamics of the network. These are different from the fast modes, which follow from the Rouse-like dynamics of chains between entanglements. An alternative approach to long-time relaxation behavior is to consider the motions of the junction points as reptation-like processes in a highly entangled network structure (23).

A number of studies have described translational dynamics of cross-link junctions in polymer networks through measurements of  $^2\text{H}$  nmr (30-33), nmr free induction decay (34) and neutron spin echo (35-37). In addition, rotational dynamics of cross-link junctions have been studied with magic angle spinning nmr (38,39) and time resolved fluorescence depolarization (40,41). Litvinov and Spiess (42,43) used pulsed  $^2\text{H}$  nmr to study the molecular mobility of PDMS chain segments in the filled PDMS networks. They concluded that this mobility is lower than in the bulk of the polymer matrix and decreases with deformation. Sotta and Deloche (30,31) performed  $^2\text{H}$  nmr measurements on strained PDMS networks and found the junction fluctuations to depend upon the chain length.

The neutron spin echo technique has been applied to study diffusive motions of the tetrafunctional cross-links in endlinked PDMS chains directly. Ewen and Richter (35-37,44) labeled the chain ends of uncross-linked chains dissolved in the network and the cross-links. They observed both time-independent as well as time-dependent components to the diffusive motion, so there is a finite probability of finding the cross-link at its original position. The time dependency is interpreted in terms of spatial limitations to the diffusive motion of cross-links. The authors concluded that the range of fluctuations they observed is between the prediction of the phantom network and that of the constrained junction theory, and obeys in a qualitative way the prediction by Warner.

### Poly(dimethyl siloxane) - Silica Composites

The molecular origin of the reinforcing effect of the silica in filled elastomers is not completely understood.  $^2\text{H}$  nmr studies (42,43) have shown that the dynamics of polymer segments are strongly dependent upon the surface activity of the silica. Surface hydroxylation of silica has been extensively studied (45). The predominant types of surface silanols are adjacent hydrogen bonded and isolated silanols. Both types are hydrophilic, with the isolated moieties being more reactive. If the silica surface is hydrophilic, an adsorption layer exists around the silica particle that is between 10 and 20 Å thick. Even above the glass transition temperature, the motions of the chain segments are severely limited in this boundary region, whereas outside this region they are mobile. In the following, we comment on the interfacial aspects of silica-filled elastomers, whether resulting from mixing of pre-formed silica or generation *in situ* by sol-gel precipitation. Later, we present results on dansyl-labeled cross-links that demonstrate the existence of two populations of chromophores in sol-gel derived nanocomposites: one tightly immobilized and one mobile.

Silica fillers increase the number of topological interaction sites in PDMS composite systems in a variety of ways (1,4,45-48). For example, if the PDMS has a functional silanol chain end, a condensation reaction can occur with a surface silanol, covalently endlinking the PDMS chain to the silica particle. Hydrogen bonds may also be formed between the lone pair electrons of the siloxane oxygens and the surface silanols. In addition, physical interactions between the PDMS and the silica surface may be important for highly convoluted surfaces. Finally, filler-filler interactions could occur between particles due to surface silanol condensation.

The modulus of a filled elastomer depends strongly on the amount, shape and the chemical nature of the filler phase. Although a detailed theory of stress distribution in a heterogeneously filled polymer network does not exist, a number of models have been proposed. The oldest explanation of the reinforcing effect is that the fillers contribute to an increased viscosity of the polymer medium (49). In another approach, the modulus was found to be a quadratic function of the effective filler volume fraction (50). In a sample under stress, it is believed that surface-adsorbed chain segments move relative to the surface in a detachment and subsequent reattachment process referred to as "saltation" (49).

Recently, the *in situ* precipitation of silica and other inorganic phases in different polymer matrices has been reported (6,8,51-56). This technique involves the hydrolysis and condensation of alkoxysilanes inside a polymer matrix in the presence of a catalyst. The magnitude of the reinforcing effect depends on the structure and dispersion of the silica phase. One important factor that determines the structure of the inorganic phase is the pH of the catalyst solution, since the relative rates of hydrolysis and condensation change with pH (54). High pH catalyst solutions result in discrete spherical silica particles, whereas low pH solutions result in network-like silica structures interpenetrating the polymer matrix (52-59).

The structure of these composite materials has been investigated by dielectric spectroscopy (55,56), electron microscopy (53), small angle X-ray scattering (8,54,59-61), X-ray photoelectron spectroscopy (61),  $^{29}\text{Si}$  nmr (62) and dynamic mechanical spectroscopy (55). The increase in modulus in silica-siloxane nanocomposites that is associated with the introduction of the silica phase is not clearly correlated with the observed morphology of this phase. Moreover, the role that the crosslinks and chain segments play during the nucleation and growth of the silica phase is unknown. .

## EXPERIMENTAL

Two types of labeled PDMS were prepared for study of cross-link rotational diffusion and for probing of local structure in nanocomposites. Both types of networks were based on hydroxy-terminated PDMS of Mn 4,300, 15,200 or 28,600 that were end-linked at room temperature using a chromophore-labeled triethoxysilane and a tin octoate catalyst. For the rotational diffusion studies, a cross-linker mixture was prepared containing 99.9 mole% methyl triethoxy silane (MTES), which was purchased from Huls-Petrarch, and 0.1 mole% naphthyltriethoxysilane (NTES), which was prepared by a Grignard reaction between 2-bromonaphthalene and a 10-fold excess of tetraethoxysilane (63). At high naphthalene concentrations there is a possibility of fluorescence anisotropy decay due to excitation energy transfer (EET) (64,65). However, we have shown (63) that there is no anisotropy decay due to EET in the networks prepared under these conditions. Dansyl-labeled networks were prepared in an analogous fashion for our studies on nanocomposites, except that we used N-(triethoxysilylpropyl)dansylamide (DTES), which was obtained from Huls-Petrarch.

In both sets of samples, the precursor mixture was cured at room temperature under nitrogen for 48 hours at a relative humidity of 15%, followed by 72 hours under vacuum. The samples were then swollen in tetrahydrofuran (THF) for 72 hours to extract all unreacted materials. Next, increasing amounts of methanol were added to deswell the samples until they were swollen in pure methanol. Finally, the samples were dried in air for 48 hours and in vacuum for 48 hours. Figure 1 schematically shows both types of labeled cross-link junctions. Note that the ratio of the molar concentration of ethoxy groups on the cross-linking species to the concentration of terminal silanol groups on the PDMS chains, which we refer to as the excess ratio  $r$ , is closely related to the cross-link size and functionality. We have demonstrated (63) that substantial self-condensation of the cross-linking precursor occurs. In the absence of this phenomenon, no network will form at all at higher  $r$  ratios. We have also attempted to estimate the average cross-link size and functionality  $f$  of the resulting networks (67).

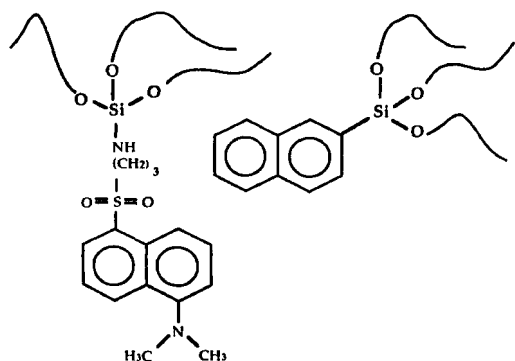


**Figure 1.** The probe molecules dansylpropylamide and naphthalene bound to trifunctional cross-link junctions.

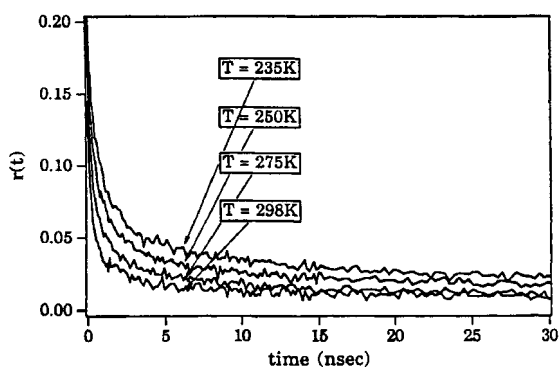


**Figure 2.** Naphthalene fluorescence anisotropy as a function of time at different temperatures, from the network with  $M_c = 15,200$  and  $r = 10$ .

Silica was precipitated inside dansyl-labeled PDMS networks by standard sol-gel procedures. The PDMS networks were prepared with  $r = 2.0$  and with the dansyl chromophore bound to 0.1% of the cross-links. Extracted network samples were swollen in tetraethoxysilane (TEOS), 50 vol% TEOS/50 vol% MTES, MTES and 50 vol% MTES/50 vol% dimethyl diethoxysilane (DMDES). The swollen samples were then placed in aqueous solutions of ethylamine (pH = 12.1) for 2 hours. Subsequently, the samples were dried in air and then extracted for seven days in THF that was periodically renewed. The samples were deswelled by adding increasing fractions of methanol to the THF. Finally, the samples were dried in air for 48 hours and in vacuum for 48 hours.

The instrumentation that was used to measure the time-dependent and photostationary fluorescence emission has been described elsewhere (40,41,63-67,80,87).

## RESULTS

### Dynamics of Crosslink Mobility in Poly(dimethyl siloxane) Networks

Above the melting temperature of the PDMS (190K) the rubber network is in the amorphous state and the polymer backbone undergoes random Brownian motion. As a result of this, the crosslink junctions will both translate and rotate as will the attached naphthalene chromophores. If this reorientation occurs during the excited state lifetime of the chromophore, the fluorescence anisotropy will decay with a

characteristic relaxation time that will be correlated with the crosslink motion. For unrestricted motion of the chromophore, the rotational diffusion coefficient  $D$  will be simply related to the rotational relaxation time  $T$  through  $D = 1/6T$ . For polymer (68,69) or micelle systems (70), however, the observed relaxation behavior is explained using a two-step model, with a fast and a slow orientational relaxation superimposed.

We have prepared a series of networks with  $M_n = 15,200$  and  $r$  varying between 0.7 and 20 and found that the anisotropy decay decays more slowly as  $r$  increases. We have also kept  $r$  constant at 1 and varied the molecular weight of the PDMS precursor chain from 4,300 to 28,600. We have interpreted our data (63) in terms of a "wobbling in a cone" model in which we assume that the fast relaxation process corresponds to the anisotropic naphthalene probe rapidly moving within a restricted region that is imposed by local geometry surrounding the crosslink junction, whereas the slow relaxation process consists of an unrestricted motion that leads to complete reorientation. We found that the slow diffusion coefficient  $D_{slow}$  was independent of molecular weight, but that the fast component  $D_w$  decreased as the molecular weight between crosslinks increased. At 298K the cone angle reflecting the local restrictions to motion decreased from  $50^\circ$  for  $M_c = 28,600$  to  $40^\circ$  for  $M_c = 4,300$ .

We determined the fluorescence anisotropy decay of all samples over a temperature range from 235K to 298K. Below 235 K the appearance of crystallites causes scattering which leads to additional depolarization. In Fig. 2 we show, for example, the anisotropy decay of the sample prepared with excess ratio  $r = 10$  at temperatures  $T = 298, 275, 250$  and  $235$ K. The decay slows down markedly with decreasing temperature. We fit the decay curves to a multiexponential function and obtain the fast diffusion constant for the constrained wobbling,  $D_w$ , the slow diffusion constant associated with the complete reorientation,  $D_{slow}$ , and the restricted cone angle. For the sample prepared with  $r = 10$ , we plot these diffusion constants as a function of  $1/T$  in Fig. 3. A semi-logarithmic dependence between these quantities indicates an Arrhenius relationship for the diffusion constants. Similar results were obtained for samples with different excess ratios. The activation energies for both diffusion constants were  $11.0 \pm 1.4$  kJ/mole in all samples. Over the range of  $r = 0.7$  to  $r = 20$ , these activation energies are independent of  $r$ , within experimental error (63).

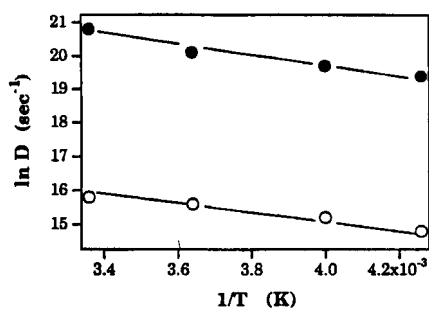


**Figure 3** The diffusion constants  $D_w$  and  $D_{slow}$ , as a function of reciprocal temperature  $1/T$ ; network with  $M_c = 15,200$  and  $r = 10$ . Taken from Ref. (63).

●  $D_w$       ○  $D_{slow}$

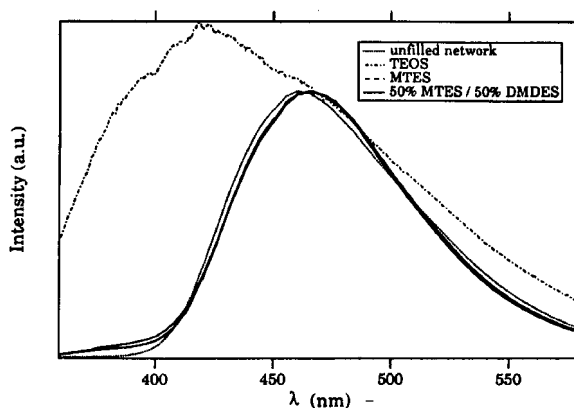


**Figure 4.** Dansyl fluorescence emission spectra of PDMS/silica nanocomposites in which silica has been precipitated from various precursor mixtures; excited at  $\lambda_{exc} = 340$  nm.

No quantitative network model is available to describe the rotational diffusion rate of cross-links. Previously, a qualitative mechanism was proposed by which the orientational correlation of labeled cross-links decays (71). This model is based on the notion that each of the  $f$  multiple chains emanating from a junction experiences a range of motions and exerts a corresponding torque on the cross-link junction. The spatial requirements of chain-like multifunctional junctions in PDMS networks have been analyzed by Flory (14). The chains emanating from a junction occupy approximately half of the space they pervade when they are randomly configured. Polymer segments that are involved in cross-link reorientation are stretched beyond their undeformed dimensions. As a result, some conformational changes leading to cross-link reorientation are hindered. Hence, the cross-link creates local density fluctuations in the network polymer (72-76), allowing restricted-angle rotations of the naphthalene transition dipole moment.

All of the experimental results (63) support the importance of local free volume effects in the vicinity of the cross-link junction: 1) From the molecular weight dependence of  $D_{slow}$  in networks prepared with

$r = 1$ , we find that fewer than approximately 60 repeating units are responsible for complete rotation of a cross-link junction. This is significantly lower than the approximately 115 repeating units corresponding to the PDMS entanglement molecular weight of 8,000. 2) At a given temperature, increasing  $r$  and hence increasing the average cross-link size decreases  $D_{\text{slow}}$  of the bound probe substantially. However,  $D_w$  is independent of  $r$  suggesting that there is a constant amount of void volume adjacent to the cross-links. 3) Reorientation of the NTES probe dissolved in an unlabeled network slows down relative to the bound probe. Since the activation energy for rotation is the same in both cases, we argue that the relevant polymer motions are the same, but that local packing differs and is tighter around a probe that is randomly dispersed. 4) Swelling the network in a low viscosity PDMS oil slows down the slow reorientation of the probe. We attribute this to decreased rotational freedom of the  $f$  strained chains emanating from a labeled cross-link junction. 5) The temperature dependence of the decay constants for all samples indicate Arrhenius activated rotational motion of the cross-links.

#### Interfacial Effects in Poly(dimethyl siloxane) - Silica Nanocomposites

Through observation of the steady state fluorescence of dansyl groups covalently bound to a small percentage of the crosslink junctions, we monitor the local structure of *in-situ* formed nanocomposites in the vicinity of the cross-links. Dansyl is a fluorescent dye that is mainly used as a solvatochromic probe, for which changes in emission band position indicate changes in polarity of the surrounding medium. Because of this solvatochromic behavior, dansyl has been used to probe the microenvironment in synthetic polymer systems (77-82), self-organizing systems (83) and surfaces (84-86). Recently, we have shown (87) that dansyl can also be used as a rigidochromic probe that can monitor the local viscosity. This property is closely related to the twisted intramolecular charge transfer character of 1-aminonaphthalenes in the excited state (87-89).

We have investigated the local matrix mobility surrounding the dansyl probes as a function of time of immersion in the catalyst solution, type of catalyst, pH of catalyst solution and degree of swelling in different solvents (87). In addition, we precipitated various silicon oxides inside the PDMS matrix from different alkoxy silane precursors. In Fig. 4, we show the dansyl fluorescence spectra of three siloxane networks in which we precipitated silicon oxides from TEOS, MTES and 50% MTES/50% DMDES. These are normalized to coincide at 460 nm. Corresponding small angle X-ray scattering data indicate that the silica particles precipitated from TEOS in ethyl amine solution are spherical and have a smooth interface (87). In Table I, we show the structure and swelling properties of these three composites along with those of the unfilled network.

From Fig. 4 it can be seen that only the silica phase precipitated from TEOS changes the local viscosity. The phases precipitated from MTES/DMDES do not. We also obtained an emission spectrum from the labeled unfilled PDMS "starting" material. We subtracted this spectrum from the spectra that we show in Fig. 4. In the case of TEOS-derived nanocomposites, a single high-energy band results from this spectral subtraction (87). We interpret this as an indication of a distinct population of cross-link bound dansyl moieties that experiences a much more rigid environment than in the unfilled PDMS. The absence of this high energy band in the MTES and MTES/DMDES spectra indicates that more of the labeled cross-links experience a significant increase in the local viscosity. Associated with this, we see in Table 1 a sharp increase in the THF uptake as we increase the methyl-content of the precipitated phase. We postulate that the silica phase inside these two samples is coated with methyl groups, which prevents strong interactions such as found for TEOS-derived silica. By increasing the methyl-content of the silica precursor, we effectively reduce silica-siloxane interactions and, thus, reduce the nanocomposite modulus.

**Table 1.** Composition and swelling properties of the nanocomposite samples.

precipitant	$w_{\text{in}}$	$w_2$ in THF
- (unfilled)	0.000	0.160
TEOS	0.303	0.493
50 vol% TEOS + 50 vol% MTES	0.208	0.402
MTES	0.185	0.233
50 vol% MTES + 50 vol% DMDES	0.116	0.189

#### SUMMARY

To summarize the dynamic results from the fluorescence depolarization measurements, both fast and slower probe motion are caused by similar type of network segmental polymer motions, but the differences are related to the distance scale of these rotations. Wobbling in a cone is driven by constrained localized motions of the bonds immediately adjacent to the probe. The slower, complete reorientation is driven by cooperative motions of a larger chain segments connected to the cross-link.

Steric constraints in the immediate vicinity of the probe have no influence on Dslow. However, the slower diffusion is still "local", since complete reorientation of the labeled cross-links involves molecular weights smaller than the entanglement molecular weight.

The most significant discovery of the nanocomposite results is the existence of two populations of chromophores, based on the application of the rigidochromic aspects of the dansyl probe. One population is bound rather rigidly, presumably as a result of strong interactions with the polar interface of the inorganic domains. The second population is characteristic of the labeled elastomer network. Given the importance of the cross-link junction fluctuations to the bulk properties of elastomer systems, the sensitivity of the naphthyl and dansyl probes for the direct study of the junction dynamics and local environment makes this a particularly good combination of functional dye photophysics and materials science. Research is continuing with different functional dyes, alternate attachment schemes and other organic/inorganic nanocomposite systems.

**ACKNOWLEDGEMENT** This work was supported by Ford Motor Corporation and Hitachi, Ltd.

## REFERENCES

1. W.Noll, *Chemistry and Technology of Silicones*, Academic Press: New York, 702, 1968.
2. C.P.Wong, Ed., *Polymers for Electronic and Photonic Applications*, Academic Press: San Diego, 1993.
3. J.E.Mark in *Inorganic Polymers*; J.E.Mark, H.R.Allcock and R.West, Eds.; Prentice Hall: Englewood Cliffs, 1992.
4. K.E.Polmanteer and C.W.Lentz, *Rubber Chem. Tech.* **48**, 795, 1975.
5. B.J.Brisdon, B.R.Heywood, A.G.W.Hodson, S.Mann and K.K.W.Wong, *Adv. Mater.* **5**, 49, 1993.
6. B.M.Novak, *Adv. Mater.* **5**, 422, 1993.
7. C.J.Brinker, G.W.Scherer, *Sol-Gel Science*, Academic Press: New York, 1990.
8. D.W.Schaefer, J.E.Mark, D.McCarthy, L.Jian, C.-C.Sun and B.Farago in *Polymer Based Composites*; D.W.Schaeffer and J.E.Mark, Eds., Materials Research Society: **171**, 57, 1990.
9. D.W.Schaefer, J.E.Mark, C.-C.Sun, D.W.McCarthy, C.-Y.Jiang, Y.-P.Ning, S.Spooner in *Ultrastructure Processing of Advanced Materials*, D.R.Uhlmann and D.R.Ulrich, Eds.; John Wiley & Sons, Inc.: New York, 1992.
10. J.E.Mark and B.Erman, *Rubberlike Elasticity, a Molecular Primer*, John Wiley and Sons: New York, 1988.
11. P.J.Flory, *J. Chem. Phys.* **66**, 5720, 1977.
12. P.J.Flory and B.Erman, *Macromol.* **15**, 1982.
13. P.J.Flory, *Macromol.* **12**, 119, 1979.
14. P.J.Flory and B.Erman, *J. Polym. Sci., Polym. Phys.* **22**, 49, 1984.
15. L.M.Dossin and W.W.Graessley, *Macromol.* **12**, 123, 1979.
16. M.Gottlieb and R.J.Gaylord, *Macromol.* **17**, 2024, 1984.
17. M.Doi and S.F.Edwards, *The Theory of Polymer Dynamics*, Oxford University Press: Oxford, 1986.
18. S.F.Edwards and Th.Vilgis, *Polymer* **27**, 483, 1986.
19. B.E.Eichinger, *Ann. Rev. Phys. Chem.* **34**, 359, 1983.
20. R.T.Deam and S.F.Edwards, *Philosoph. Trans. R. Soc. London* **280**, 317, 1976.
21. T.A.Vilgis in *Elastomeric Polymer Networks*; J.E.Mark and B.Erman, Eds., Prentice Hall: Englewood Cliffs, 32, 1992.
22. M.D.Ediger, *Ann. Rev. Phys. Chem.* **42**, 225, 1991.
23. G.Heinrich and T.A.Vilgis, *Macromol.* **25**, 404, 1992.
24. M.Warner, *The Connectivity of Polymer Networks by Neutron Scattering*, Rutherford Appleton Laboratory, London, 1982.
25. M.Warner, *J. Phys. C: Solid State Phys.* **14**, 4985, 1981.
26. M.Warner and S.F.Edwards, *J. Phys. A: Math. Gen.* **11**, 1649, 1978.
27. J.S.Higgins, K.Ma and R.H.Hall, *J. Phys.C: Solid State Phys.* **14**, 4995, 1981.
28. J.G.Curro and P.Pincus, *Macromol.* **16**, 559, 1983.
29. N.A.Neuburger and B.E.Eichinger, *J. Chem. Phys.* **83**, 884, 1985.
30. P.Sotta and B.Deloche, *J.Chem.Phys.* **100**, 4591, 1994.
31. P.Sotta and B.Deloche, *Macromol.* **23**, 1999, 1990.
32. M.G.Brereton, *Macromol.* **24**, 6160, 1991.
33. M.G.Brereton, *Progr. Coll. Polym. Sci.* **90**, 90, 1992.
34. T.P.Kulagina, V.M.Litvinov and K.T.Summanen, *J. Polym. Sci.: Part B: Polym. Phys.* **31**, 241, 1993.
35. R.Oeser, B.Ewen, D.Richter and B.Farago, *Phys. Rev. Lett.* **60**, 1041, 1988.

36. B.Ewen and D.Richter. in *Elastomeric Polymer Networks*, J.E.Mark and B.Erman, Eds.; Prentice Hall: Englewood Cliffs, 220, 1990.
37. B.Ewen and D.Richter in *Molecular Basis of Polymer Networks*, A. Baumgartner, Ed., Springer Verlag: Berlin, 42, 1989.
38. J.-F.Shi, L.C.Dickinson, W.J.MacKnight, J.C.W.Chien, C.Zhang, Y.Liu, Y.Chin, A.A.Jones and P.T.Inglefield, *Macromol.* **26**, 1008, 1993.
39. J.-F.Shi, L.C.Dickinson, W.J.MacKnight and J.C.W.Chien, *Macromol.* **26**, 5908, 1993.
40. A.D.Stein, D.A.Hoffmann, C.W.Frank and M.D.Fayer, *J. Chem. Phys.* **96**, 3269, 1992.
41. D.A.Hoffmann, A.D.Stein, J.E.Anderson, M.D.Fayer and C.W.Frank, in preparation.
42. V.M.Litvinov and H.W.Spiess, *Makromol. Chem.* **192**, 3005, 1991.
43. V.M.Litvinov and H.W.Spiess, *Makromol. Chem.* **193**, 1184, 1992.
44. A.J.Staverman in *Elastomeric Polymer Networks*; J.E.Mark and B.Erman, Eds. Prentice-Hall: Englewood Cliffs, 6, 1992.
45. E.M.Dannenberg, *Rubber Chem. Tech.* **48**, 410, 1975.
46. B.B.Boonstra, H.Cochrane and E.M.Dannenberg, *Rubber Chem. Tech.* **48**, 558, 1975.
47. J.B.Donnet and A.Vidal in *Adv. Polym. Sci.*, K.Dusek, Ed. **76**, 1986.
48. E.P.Plueddemann *Silane Coupling Agent*, 2 ed., Plenum Press: New York, 253, 1989.
49. A.Rigbi, *Adv. Polym. Sci.* **36**, 21, 1980.
50. S.Wolff and J.B.Donnet, *Rubber Chem. Tech.* **63**, 32, 1989.
51. C.-Y.Jiang and J.E. Mark, *Makromol. Chem.*, **185**, 2609, 1984.
52. J.E.Mark and D.W. Schaefer in *Polymer Based Composites*, D.W.Schaefer and J.E.Mark, Eds., Materials Research Society, Pittsburgh **171**, 51, 1990.
53. Y.-P.Ning and J.E.Mark, *Polym. Bull.* **12**, 407, 1984.
54. G.L.Wilkes, H.H.Huang and R.H.Glaser in *Silicon-Based Polymer Science, A Comprehensive Resource*; J. M.Zeigler and F.W.G.Fearon, Eds., American Chemical Society, Washington, D.C. **224**, 207, 1990.
55. C.J.Landry, B.K.Coltrain and B.K.Brady, *Polymer* **33**, 1486, 1992.
56. C.J.Landry, B.K.Coltrain, J.A.Wesson, N.Zumbulyades and J.L.Lippert, *Polymer* **33**, 1496, 1992.
57. J.E.Mark and Y.-P.Ning, *Polym.Bull.* **12**, 413, 1984.
58. Y.-P.Ning and J.E. Mark, *Polym.Eng.Sci.* **26**, 167, 1986.
59. D.W.Schaefer, J.E.Mark, C.-C.Sun, D.W.McCarthy, C.-Y.Jiang, Y.-P.Ning and S.Spooner in *Ultrastructure Processing of Advanced Materials*; ; D.R.Uhlmann and D.R.Ulrich, Eds. John Wiley & Sons, New York, 1992.
60. P.Xu, S.Wang and J.E.Mark in *Better Ceramics Through Chemistry IV*; ; B.J.J.Zelinski, C.J.Brinker, D.E.Clark and D.R.Ulrich, Eds., Materials Research Society, Pittsburgh **180**, 446, 1990.
61. M.Nandi, J.A. Conklin, L.Salvati and A.Sen, *Chem. Mater.* **3**, 201, 1991.
62. T.Iwamoto, K.Morita and J.D.Mackenzie, *J. Non. Cryst. Sol.* **159**, 65, 1993.
63. P.B.Leezenberg, A.H.Marcus, C.W.Frank and M.D.Fayer, *J. Phys. Chem.*, submitted.
64. K.A.Peterson, A.D.Stein and M.D.Fayer, *Macromol.* **23**, 111, 1990.
65. A.D.Stein, K.A.Peterson and M.D.Fayer, *J. Chem. Phys.* **92**, 5622, 1990.
66. N.A.Diachun, A.H.Marcus, D.M.Hussey and M.D.Fayer, *J. Am. Chem. Soc.* **116**, 1027, 1994.
67. P.B.Leezenberg, PhD Dissertation, Stanford University, 1994.
68. A.Szabo, *J. Chem. Phys.* **81**, 150, 1984.
69. A.C.Ouano and R.Pecora, *Macromol.* **13**, 1173, 1980.
70. E.L.Quitevis, A.H.Marcus and M.D.Fayer, *J. Phys. Chem.* **97**, 5762, 1993.
71. A.D.Stein, D.A.Hoffmann, C.W.Frank and M.D.Fayer, *J. Chem. Phys.* **96**, 3269, 1992.
72. V.K.Soni and R.S. Stein, *Macromol.* **23**, 5257, 1990.
73. S.F.Mallam, F.Horkay, A.Hecht, A.R.Rennie and E.Geissler, *Macromol.* **24**, 543, 1991.
74. S.F.Mallam, A.M. Hecht and E. Geissler, *J. Chem. Phys.* **91**, 6447, 1989.
75. E.F.Geissler, F.Horkay, A.M.Hecht and M.Zrinyi, *J. Chem. Phys.*, **90**, 1924, 1989.
76. A.M.Hecht, A.Gullermo, F.Horkay, S.F.Mallam, J.F.Legrand and E.Geissler, *Macromol.* **25**, 3677, 1992.
77. D.A.Hoffmann, J.E.Anderson and C.W.Frank, *J. Mat. Chem.* **1995**.
78. Y.Hu, K.Horie and H.Ushiki, *Macromol.* **25**, 6040, 1992.
79. Y.Hu, K.Horie, H.Ushiki, F.Tsunomori and T.Yamashita, *Macromol.* **25**, 7324, 1992.
80. P.B.Leezenberg and C.W.Frank *Macromol.*, submitted
81. K.J.Shea and G.J. Stoddard, *Macromol.* **24**, 1207, 1991.
82. K.J.Shea, G.J.Stoddard, D.M.Shavelle, F.Wakui and R.M.Choate, *Macromol.* **23**, 4497, 1990.
83. T.Seo, S.Take, K.Miwa, K.Hamada and T. Ijima, *Macromol.* **24**, 4255, 1991.
84. S.R.Holmes-Farley and G.M. Whitesides, *Langmuir.* **2**, 266, 1986.
85. C.H.Lochmuller, D.B.Marshall and D.R.Wilder, *Anal. Chim. Acta* **130**, 31, 1981.
86. C.H.Lochmuller, D.B.Marshall and J.M.Harris, *Anal. Chim. Acta* **131**, 263, 1981.
87. P.B.Leezenberg and C.W.Frank *Chem. Mater.*, in press, 1995.
88. K.P.Ghigginio, A.G.Lee, S.R.Meech, D.V.O'Connor and D.Phillips, *Biochem.* **20**, 5381, 1981.
89. S.R.Meech, D.V.O'Connor and D.Phillips, *J. Chem. Soc., Faraday Trans. 2* **79**, 1563, 1983.